NASA Technical Memorandum 79042

FEASIBILITY OF WING SHIELDING OF THE AIRPLANE INTERIOR FROM THE SHOCK NOISE GENERATED BY SUPERSONIC TIP SPEED PROPELLERS

James H. Dittmar
Lewis Research Center
Cleveland, Ohio

December 1978

SUMMARY

A high tip speed turboprop is being considered as a future energy conservative airplane. The high tip speed of the propeller, combined with the cruise speed of the airplane, results in supersonic relative flow on the propeller tips. These supersonic blade sections could generate noise that is a cabin environment problem. This report investigates the feasibility of using wing shielding to lessen the impact of this supersonic propeller noise. An analytical model is chosen which considers that shock waves are associated with the propeller tip flow and indicates how they would be prevented from impinging on the airplane fuselage. An example calculation is performed where a swept wing is used to shield the fuselage from significant portions of the propeller shock waves.

INTRODUCTION

One of the candidate engines for a future energy conservative airplane is a high tip speed turboprop. The high tip speed of the propeller, combined with the high subsonic cruise Mach number of the airplane, results in supersonic relative velocities over the outer portions of the propeller blades. During airplane cruise these supersonic blade sections generate significant noise that might become a cabin environment noise problem.

The intent of this report is to investigate the feasibility of using wing shielding to lessen the impact of this supersonic propeller noise on the airplane interior. An analytical model is chosen which considers that shock waves are associated with the propeller tip flow and attempts to trace how they could be blocked from impinging on the airplane fuselage. An example is considered in which a swept wing is used to shield the fuselage from significant portions of the propeller shock waves. This report does not attempt to address the other sources of high speed propeller noise such as those addressed by Hanson (ref. 1) and Farassat (ref. 2) but only deals with the shock waves associated with the propeller tip.

MODEL

In order to determine the feasibility of wing shielding for reducing the airplane interior noise of a high tip speed turboprop, a particular airplane type has been chosen. This is a high wing airplane with the engines in nacelles on the wing as shown in figure 1. (A low wing aircraft could be designed to have similar shielding, but the high wing would have less problems with landing gear height.)

In the modeling it is assumed that some portion of the tip of the propeller is operating supersonically when the plane is at cruise. The supersonic pro-

peller tip section is assumed to have attached shock waves on both the pressure and suction surfaces. A sketch of the propeller tip might look as in figure 2 which is a view of the tip looking toward the hub.

The shock wave pattern has leading and trailing edge shocks. The angle between the shock wave and the blade camberline is θ. (A list of symbols is included in appendix A.) In figure 2 the shock waves are shown to have different angles, θ_1 and θ_2. In the text of this report the angle θ could be construed as being either the leading or trailing edge shock. However since the leading edge shock is typically stronger and thus represents a more critical shielding problem, the leading edge shock geometry and angle are used in the following development and in the sample calculations.

These propeller tip shock waves rotate with the propeller and would impinge upon the airplane fuselage creating an interior noise problem. In order to illustrate the possibility of using the wing to block these waves a number of head-on airplane sketches are shown in figure 3. These drawings illustrate a propeller blade in various positions and indicate the position of the shock wave from the suction surface of the propeller. The blocking of the suction wave is shown here for purposes of illustration and it will be shown later that the pressure wave can be made to pass behind the airplane. The shock wave is assumed to lie in a plane which is perpendicular to the blade span. The blade is shown as being the same from hub to tip only for ease of illustration.

As can be observed in figure 3 the suction surface shock wave strikes the fuselage only when the propeller blade is in a certain portion of its rotation. In particular this occurs when the blade is located in the quadrant of the propeller rotation which is above the airplane wing. Therefore portions of the airplane fuselage may be shielded from these suction surface shock waves by the presence of the wing. The intent in this report is to investigate the geometric aspects of this wing shielding and to evaluate the possibility of using this wing shielding effect to minimize the shock wave noise reaching the fuselage.

Shock Wave Model

The shock wave model that is used in this report is presented in detail in reference 3. This model is valid for the relatively small angles of attack, which are characteristic of the supersonic tip sections of a high speed turboprop. In chart 2 (ref. 3) the leading edge shock wave angle (θ) for an attached shock is given in terms of the deflection angle at the leading edge (δ, the blade semi-vertex angle) and the upstream Mach number relative to the blade. This geometry was shown in figure 2.

Figure 4 is a sketch of the supersonic blade section and μ is its angle with respect to the centerline of the engine. The pressure and suction waves

make angles γ_P and γ_S with the centerline of the engine. In this geometry

$$\gamma_P = \pi - (\theta_P - \mu) \tag{1}$$

$$\gamma_S = \pi - \theta_S - \mu \tag{2}$$

The angle of each of the attached shocks with respect to the blade is then obtainable by using reference 3 to determine the angles θ_P and θ_S and equations 1 and 2 are used to determine the angles with respect to the engine centerline.

Shielding Geometry Model

The airplane geometry chosen for investigating this wing shielding feasibility is shown in figures 1 and 5. In figure 5(a) the high wing airplane is viewed head-on and the fuselage cross-section is represented by a circle of radius R_f. The propeller has an outer radius R_o and has its center in the plane of the wing and at a horizontal distance h from the fuselage center. The propeller centerline is chosen to lie along the z axis of the x-y-z coorindate system which is shown in figure 5(b). The angle Φ is measured from the x axis in a clockwise direction.

The position of both the suction and pressure waves, called S and P, can be determined as vectors originating from the blade section. For ease in determining these vectors it is assumed that no radial flows exist over the blade surface and therefore the shock waves are in a plane which is perpendicular to the blade span. Using figures 4 and 5 the two vectors can be expressed

$$\vec{P} = |P| \, (-\sin\gamma_P \sin\Phi \, \hat{i} + \sin\gamma_P \cos\Phi \, \hat{j} - \cos\gamma_P \hat{k}) \tag{3}$$

$$\vec{S} = |S| \, (\sin\gamma_S \sin\Phi \, \hat{i} - \sin\gamma_S \cos\Phi \, \hat{j} - \cos\gamma_S \hat{k}) \tag{4}$$

where $|S|$ and $|P|$ are the length of vectors $\vec{S}$ and $\vec{P}$ and $\hat{i}$, $\hat{j}$, $\hat{k}$ are the unit vectors in the x, y and z directions. The origin of these vectors is on the blade at some radius r and with the blade at some angle Φ in its rotation.

In order to made the problem more tractable the assumption is made that this shock wave which leaves the blade at position Φ continues in the same direction which it started. In other words the wave continues to travel in the plane which is perpendicular to the blade span when the blade was at angle Φ and it continues to make the same angles with respect to the x, y and z axis. This then enables the geometric construction of figure 6 and the determination of the range of blade angles Φ where the wave will strike the fuselage.

Figure 6(a) shows the range of angles where the S wave would strike an infinitely long cylindrical fuselage. Figure 6(b) indicates the boundaries for the P wave. As can be observed, only a small portion of a revolution of the blade is of concern. The angles that bound these ranges can be determined from the airplane geometry and are derived in appendix B. The initial S wave angle is indicated as Φ_{S_i} the final angle as Φ_{S_f} and Φ_{P_i} and Φ_{P_f} are used for the P wave angles. These angles are given by the following equations.

$$\Phi_{S_i} = 2\pi - \tan^{-1}\left(\frac{R_f}{h}\right) - \sin^{-1}\left[\frac{R_f + r}{\sqrt{R_f^2 + h^2}}\right] \tag{5}$$

$$\Phi_{S_f} = 2\pi - \tan^{-1}\left(\frac{R_f}{h}\right) + \sin^{-1}\left[\frac{R_f - r}{\sqrt{R_f^2 + h^2}}\right] \tag{6}$$

$$\Phi_{P_i} = \pi - \tan^{-1}\left(\frac{R_f}{h}\right) - \sin^{-1}\left[\frac{R_f - r}{\sqrt{R_f^2 + h^2}}\right] \tag{7}$$

$$\Phi_{P_f} = \pi - \tan^{-1}\left(\frac{R_f}{h}\right) + \sin^{-1}\left[\frac{R_f + r}{\sqrt{R_f^2 + h^2}}\right] \tag{8}$$

where R_f is the fuselage radius, r is the radial location of the shock on the blade section and h is the horizontal distance from the fuselage center to the propeller center.

In figure 7 it is illustrated that the typical P wave which might strike the fuselage would impact behind the wing. Here it can be seen that the key to minimizing the impact of these "P" waves is to cause them to pass behind the fuselage. With the known angle Φ_P in the rotational plane, and the vector $\vec{P}$ it is possible to calculate the projected angle of the P wave in the y-z plane. In figure 7 this is angle η. Returning to the vector expressions (eqs. 3 and 4) this angle is then the arc tangent of the minus y component divided by the z component

$$\eta = \tan^{-1}\left(\tan \gamma_P \cos \Phi_P\right) \tag{9}$$

Therefore for a given Φ_P it is possible to evaluate the angle at which the wave travels aft in the y-z plane. From the geometry of the airplane it is also possible to determine the angle (η_M) from the propeller for a wave that would just pass behind the airplane. It is

$$\eta_M = \tan^{-1} \frac{h + E}{C} \tag{10}$$

where C is the distance from the propeller plane to the rear of the fuselage, h is the horizontal distance from the propeller center to the fuselage center and E is the projected location of the propeller blade section in the y plane

$$E = r \sin \Phi_P \tag{11}$$

In theory then it is possible to choose h, the engine location, such that all of the P waves for Φ_{P_i} to Φ_{P_f} pass downstream of the airplane fuselage. Combining equations 9, 10 and 11,

$$h = C \tan \gamma_P \cos \Phi_P - r \sin \Phi_P \tag{12}$$

By setting the derivative of h with respect to Φ_P equal to zero, the smallest h can be calculated so that all of the pressure waves pass downstream. This smallest valve of h can be expressed as,

$$h_M = \sqrt{r^2 + C^2 \tan^2 \gamma_P}, \tag{13}$$

this occurs at an angle

$$\Phi_{P_M} = \tan^{-1} \left(\frac{-r}{C \tan \gamma_P} \right) . \tag{14}$$

These expressions then determine the value of h for use in future calculations of the S wave behavior.

The situation with the "S" wave is shown in figure 8(a). The intent here is to have the wing swept at an angle so as to block all the S waves from striking the fuselage. The angle ψ that an S wave makes from the propeller can be determined knowing Φ_S

$$\psi = \tan^{-1} \left(\frac{\cot \gamma_S}{\cos \Phi_S} \right) \tag{15}$$

It then becomes necessary to determine the wing which can block these waves. In figure 8(a) the tangent of the wing angle J can be determined to be

$$\tan J = \frac{A + G + B}{F - Q} \tag{16}$$

It is then necessary to find A, B, F and Q. G is the distance of the propeller tip from the leading edge of the wing and is assumed known. F is the distance in the y plane that the wave has gone when it crosses the wing. From figure 8(b)

$$F = -\frac{r}{\sin \Phi_S} \tag{17}$$

where r is the radius to the blade section.
Q is the projection of the blade section radius in the y-z plane

$$Q = -r \sin \Phi_S \tag{18}$$

B is the distance the wave has progressed forward (-z direction) when it intercepts the wing. Returning to figure 8(a)

$$B = (F - Q) \tan \psi \tag{19}$$

and

$$A = (R_o - Q) \tan J \tag{20}$$

where R_o is the outer radius of the propeller, then

$$\tan J = \frac{(R_o - Q) \tan J + G + (F - Q) \tan \psi}{(F-Q)} \tag{21}$$

which on rearranging gives

$$J = \tan^{-1}\left(\frac{G + (F - Q) \tan \psi}{F - R_o}\right) \tag{22}$$

Equation 22 defines the wing angle necessary to block the particular "S" wave. It should be noted here that during portions of the rotation the "S" wave would traverse across the top of the fuselage (see fig. 30). However, with the high wing extending above the fuselage it is felt that this would provide the necessary shielding in this area. It should also be noted that the concept requires that propellers on opposite sides of the airplane must rotate in opposite directions. There is nothing that is obviously in error if this is done but the increase in parts caused by the oppositely rotating propellers is a definite disadvantage.

It appears feasible in theory to configure this high wing airplane so that the shock wave from the pressure surface of a blade section would pass downstream of the airplane and the wave from the suction surface would be blocked by the wing

Since each section of the blade, from the tip to the sonic line, would have different shock wave angles and blade setting angles it may not be possible to block all of the waves. However, it may be possible to block significant portions of the shock waves so that the cabin noise might be appreciable reduced.

EXAMPLE

The following example illustrates how this approach might be applied to an airplane design. A sketch of the airplane is shown in figure 1 which is 27.4 m (90 ft) long with a 27.4 m (90 ft) wingspan. The fuselage is 2.44 m (8 ft) in diameter and the propellers are 2.74 m (9 ft) in diameter. The airplane propeller tips are assumed to have a relative Mach number of 1.2, achieved by an airplane Mach number of 0.85 and a propeller rotational Mach number of 0.85. The plane of the propeller is assumed to be 15.24 m (50 ft) from the rear of the airplane and the airplane is operating at 10.7 km (35 000 ft) altitude.

The first step in working this example is to determine the shock wave angles (θ) with respect to the propeller blades. The blade leading edge is assumed to have an included angle of 2°, which makes $\delta = 1^{\circ}$. The angle of attack for these blades is typically small and for ease in working the example the shock waves are assumed to be the same on each side of the blade ($\theta_P = \theta_S$). In referring to reference 3, figure 4, the shock wave will be attached to the leading edge at incoming Mach numbers of approximately 1.1 or greater. Therefore for this example an attempt will be made to adjust the airplane geometry so that the attached shock waves, those from the blade sections from the tip (M = 1.2) down to the blade position where M = 1.1, do not strike the fuselage. It should be noted here that the bow type shock waves from the sections from M = 1.1 to M = 1.0 will not be blocked from striking the fuselage. This shock noise plus the other existing propeller noise sources may still cause an interior noise problem. However, it is felt that by blocking the stronger attached shock waves a significant noise reduction would be achieved.

From chart 2 of reference 3 the shock wave angles for a 1° angle are

$$\theta_S = \theta_P = 59^{\circ} \text{ at the tip (M = 1.2)}$$

and

$$\theta_S = \theta_P = 69^{\circ} \text{ at the M = 1.1 point.}$$

At the tip the blade is set with the flow, which has both its circumferential and axial Mach numbers equal to 0.85 and thus the blade tip is set at $\mu = 45^{\circ}$. At the point where the blade is traveling at M = 1.1 (0.824 R_o), the blade is rotating at a Mach number of 0.7 and the angle $\mu = 39^{\circ}$. Using equations (1)

and (2) this then yields the following values for the shock angles

$$\gamma_{P_{tip}} = 166^{o}$$

$$\gamma_{S_{tip}} = 76^{o}$$

$$\gamma_{P_{M=1.1}} = 150^{o}$$

$$\gamma_{S_{M=1.1}} = 72^{o}$$

This indicates that for all of the blade sections, the pressure waves are propagating downstream and the suction surface waves are propagating slightly ahead of the plane of rotation.

The next step is to determine the engine position on the wing, h, that will cause the P waves for all of the sections to pass downstream of the airplane. The worst case is for the M = 1.1 point where, from equations 7 and 8, $\Phi_{P_i} = 171.6^{o}$ and $\Phi_{P_f} = 187.4^{o}$.

The calculated value of h_M is determined from equation 13 to be 8.87 m (29.1 ft). This occurs at an angle Φ_P of 187.3^{o} which is within the range of Φ_P's for this case. Therefore, it the engine is placed 8.87 m (29.1 ft) from the fuselage the P waves will all pass behind the airplane.

With this calculated value of h using equations (5), (6) and (15), for the M = 1.1 point on the blade,

$$\Phi_{S_i} = 336.9^{o} \qquad \psi_{S_i} = 19.5^{o}$$

$$\Phi_{S_f} = 352.7^{o} \qquad \psi_{S_f} = 18.1^{o}$$

and for the blade tip,

$$\Phi_{S_i} = 335.3^{o} \qquad \psi_{S_i} = 15.3^{o}$$

$$\Phi_{S_f} = 351.2^{o} \qquad \psi_{S_f} = 14.2^{o}$$

The largest sweep angle J occurs for the initial wave at the M = 1.1 point. Using equations 17, 18 and 22, with an assumed distance G of 0.61 m (2 ft), gives a sweep angle J of 44.4^{o} which would most logically be increased to 45^{o}.

In this example the attached shock waves, from the blade sections from

the tip down to the M = 1.1 location on the blade, have been prevented from directly striking the fuselage of the airplane. This was accomplished by selectively choosing the position of the engine on the wing and the sweep angle of the wing.

AN ESTIMATE OF THE ACHIEVABLE NOISE REDUCTION

The amount of noise reduction achievable from this proposed wing shielding depends on a number of factors. These include, but may not be limited to, how much the shock noise source is above the common propeller noise sources and how much the shock wave might diffract around the wing leading edge. An exact assessment of each of these factors is not presently possible. However, the following approximations indicate the possible noise reductions achievable by this wing shielding concept.

In reference 4 an attempt was made to predict the noise from a turboprop operating at a tip relative Mach number of 1.15. The method for this estimation was an extension of sonic boom predictions to this case. The method yielded a predicted overall sound pressure level of 148 dB based on this shock model. Also included in reference 4 are the predictions provided by Hamilton Standard which do not include the presence of attached shocks. This prediction yielded a value of 137 dB. The difference of 11 dB is herein assumed to be the result of the shock noise. Since this shock noise is generated mostly at the tip, it is estimated that if the shock noise from the tip section (in the example, this is from the M = 1.1 point to tip) were blocked, an 11 dB reduction in fuselage noise could occur.

During the propeller rotation some portion of the suction surface shock wave may be diffracted around the leading edge and strike the fuselage. In order to provide an estimate of the amount of diffraction that might occur, a simple barrier shielding model will be used (ref. 5).

This model is for the attenuation of a point sound source by a barrier. It is possible that more attenuation might occur for the shock wave since it is a more directional source, however this point source model shou'd yield a first approximation to the attenuation by the wing.

The attenuation for this barrier model is

$$\text{attenuation} = \left(20 \log_{10} \left(\frac{\sqrt{2\pi N_1}}{\tanh \sqrt{2\pi N_1}} \right) + 5 \right) \text{dB} \qquad (23)$$

where in the shadow zone

$$N_1 = \frac{2}{\lambda_1} (A_1 + B_1 - d_1) \tag{24}$$

λ_1 wavelength of sound, m

d_1 straight line distance between source and receiver, m

$A_1 + B_1$ shortest path length of wave travel around the barrier between the source and receiver, m

For a 2.74 m (9 ft) diameter, 10 bladed, propeller operating at a rotational Mach number of 0.85 the blade passage tone would occur around 300 hertz. The harmonics would be multiples of this frequency, 600, 900 hertz, etc. The least attenuation would occur at the lowest frequency (BPF) so this is taken as the worst case situation. For a standard atmosphere at 10.7 km (35 000 ft), the speed of sound is (297 m/sec) which gives a wavelength of the 300 hertz tone as 0.988 m (3.24 ft).

The difference in path length for a direct path and the diffracted path $(A_1 + B_1 - d_1)$ is a variable for different portions of the propeller rotation. For this estimate the average position Φ_S of the propeller when its wave might strike the fuselage is taken as 344.8° for the attached shock at M = 1.1 and a suction shock wave angle, γ_S, of 72°. The following values can be calculated using the direction cosines of the S sector from equation 4. The distance, d_1, to the fuselage is 8.03 m (26.36 ft) and the distance around the wing leading edge, $A_1 + B_1$, is 8.13 m (26.67 ft). The calculated value of N_1 then becomes 0.193. The substitution of this N_1 into equation 23 yields a predicted attenuation of approximately 8 dB.

It should be noted that this 8 dB attenuation of the BPF is for the average propeller position where the shock wave would strike the fuselage. At some positions this attenuation would be less and at other positions more than this value. Also the attenuation would be greater for the higher hamonics of the tone (2 × BPF, 3 × BPF, etc.). It should also be noted that some shielding of the nonshock related propeller noise sources would also occur. In this section estimates of the shock noise predominance over the other propeller sources and estimates of the diffraction of the blocked shocks have been used to give an indication of the noise reduction possible from this wing shielding concept. These estimates indicate that the noise reduction possible by wing shielding of the fuselage from the propeller shocks is of the order of 8 to 10 dB.

CONCLUDING REMARKS

The intent of this report was to show the feasibility of preventing portions of the shock waves, that are attached to supersonic tip speed propellers, from reaching an airplane fuselage. This was accomplished on a high wing airplane by locating the engine on the wing so that the shock wave associated with the pressure surface of the blade, passes downstream of the airplane. The shock wave on the suction side of the blade is then blocked by properly sweeping the airplane wing. An example was worked where the attached shock waves for a propeller were shielded from directly striking the fuselage. In this example it was not possible to block all of the unattached shock waves nor were the other noise sources associated with a high tip speed propeller prevented from reaching the fuselage. In addition, diffraction around the wing may limit the amount of reduction possible. However, an estimate for this example indicates that 8 to 10 dB noise reduction may be possible. In addition, for this example, raising the centerline of the propeller above the wing or adding a vertical fence to the wing between the fuselage and the propeller would probably block even more of the shock waves. In any case, the concept of preventing portions of the blade shock waves from hitting the fuselage appears feasible and if accomplished, significant reductions in the airplane interior noise might be achieved.

APPENDIX A

LIST OF SYMBOLS

A	distance, in addition to G, that wing is behind the propeller at the propeller section where the shock wave is originating (fig. 8(a))
$A_1 + B_1$	shortest path length of wave travel over the barrier between the source and receiver (eq. 24)
B	distance measured in the z direction from the intersection of the shock wave with the wing leading edge to the plane of the propeller (fig. 8(a))
C	distance from plane of propeller to rear of fuselage (fig. 7)
d_1	straight line distance between source and receiver (eq. 24)
E	projected location of propeller blade in y-z plane (eq. 11, fig. 7)
F	distance from intersection of shock wave with the wing leading edge to the propeller centerline in the y direction (fig. 8(a))
G	distance from wing leading edge to propeller plane at the closest point in the z direction (fig. 8(a))
h	horizontal distance from fuselage center to propeller center (fig. 5(a))
$\hat{i}, \hat{j}, \hat{k}$	unit vectors in the x, y, z directions
J	wing angle measured from fuselage centerline (fig. 8(a))
M	upstream Mach number with respect to propeller blade (fig. 2)
N_1	barrier attenuation parameter (eq. 24)
$\vec{P}$	pressure surface shock wave vector (eq. 3)
Q	projected location of propeller blade section in y-z plane (fig. 8(a))
R_f	fuselage radius (fig. 5(a))
R_o	outer radius of propeller (fig. 5(a))
r	radius of a point on the propeller (fig. 5(b))
$\vec{S}$	suction surface shock wave vector (eq. 4)
x, y, z	coordinate system fixed at propeller axis (fig. 5(b))
γ_P	pressure surface shock wave angle with respect to engine centerline (fig. 4)
γ_S	suction surface shock wave angle with respect to engine centerline (fig. 4)
δ	half angle of blade leading edge wedge (fig. 2)

η angle in y-z plane of pressure surface shock wave with respect to propeller centerline (fig. 7)

η_M the angle η that would pass downstream of airplane (fig. 7)

θ shock wave angle with respect to blade centerline (fig. 2)

θ_P pressure surface shock wave angle with respect to blade centerline (fig. 4)

θ_S suction surface shock wave angle with respect to blade centerline (fig. 4)

θ_1 leading edge shock wave angle with respect to blade centerline (fig. 2)

θ_2 trailing edge shock wave angle with respect to blade centerline (fig. 2)

λ_1 wavelength of sound (eq. 24)

μ angle of blade section with respect to engine centerline (fig. 4)

Φ angle of rotation for a propeller blade (fig. 5(b))

Φ_{P_f} propeller rotation angle when pressure surface shock wave would last intersect the fuselage (fig. 6)

Φ_{P_i} propeller rotation angle when pressure surface shock wave would first intersect the fuselage (fig. 6)

Φ_{S_f} propeller rotation angle when suction surface shock wave would last intersect the fuselage (fig. 6)

Φ_{S_i} propeller rotation angle when suction surface shock wave would first intersect the fuselage (fig. 6)

ψ angle in y-z plane of suction surface shock wave with respect to propeller plane (fig. 8(a))

APPENDIX B

SOLUTIONS FOR INITIAL AND FINAL BLADE POSITIONS

Solution for Φ_{S_i}

The geometry for this for this solution is found in figure B1. The dotted line $\overline{de}$ indicates the shock wave plane which is tangent to both the fuselage and propeller circles. A line $\overline{ak}$ is drawn parallel to this wave from the center of the propeller disc to the extension of the radius of the fuselage.

Two angles which have their sides perpendicular to each other are equal. Therefore since $\overline{la}$ is perpendicular to $\overline{ta}$ and $\overline{ka}$ is perpendicular to $\overline{da}$ then

$$\angle lak = \angle dat \qquad \text{(where } \angle \text{ indicates an angle)}$$

$$\angle dat = 2\pi - \Phi_{S_i}$$

$$\Phi_{S_i} = 2\pi - \angle dat = 2\pi - \angle lak$$

$$\angle lak = \angle lab + \angle bak$$

$$\angle bak = \sin^{-1}\left(\frac{R_f + r}{\sqrt{R_f^2 + h^2}}\right)$$

$$\angle lab = \tan^{-1}\frac{R_f}{h}$$

Therefore

$$\Phi_{S_i} = 2\pi - \tan^{-1}\frac{R_f}{h} - \sin^{-1}\left(\frac{R_f + r}{\sqrt{R_f^2 + h^2}}\right)$$

Solution for Φ_{S_f}

The geometry for this solution is found in figure B2. As in the solution for Φ_{S_i}, angles with mutually perpendicular sides are equal so

$$\angle dat = \angle lak$$

so

$$\Phi_{S_f} = 2\pi - \angle lak$$

$$\angle lak = \angle lab - \angle kab$$

$$\angle lab = \tan^{-1} \frac{R_f}{h}$$

$$\angle kab = \sin^{-1}\left(\frac{R_f - r}{\sqrt{R_f^2 + h^2}}\right)$$

so

$$\Phi_{S_f} = 2\pi - \tan^{-1}\left(\frac{R_f}{h}\right) + \sin^{-1}\left(\frac{R_f - r}{\sqrt{R_f^2 + h^2}}\right)$$

Solution for Φ_{P_i}

The geometry for this solution is found in figure B3. As before angles with mutually perpendicular sides are equal.

$$\angle lak = \angle dat$$

$$\Phi_{P_i} = \pi - \angle lak$$

$$\angle lak = \angle lab + \angle bak$$

$$\angle lab = \tan^{-1}\left(\frac{R_f}{h}\right)$$

$$\angle bak = \sin^{-1}\left(\frac{R_f - r}{\sqrt{R_f^2 + h^2}}\right)$$

$$\Phi_{P_i} = \pi - \tan^{-1}\left(\frac{R_f}{h}\right) - \sin^{-1}\left(\frac{R_f - r}{\sqrt{R_f^2 + h^2}}\right)$$

Solution for Φ_{P_f}

The geometry for this solution is found in figure B4. As before angles with mutually perpendicular sides are equal.

$$\angle lak = \angle dat$$

$$\Phi_{P_f} = \pi + \angle lak$$

$$\angle lak = \angle bak - \angle lab$$

$$\angle lab = \tan^{-1}\left(\frac{R_f}{h}\right)$$

$$\angle bak = \sin^{-1}\frac{R_f + r}{\sqrt{R_f^2 + h^2}}$$

$$\Phi_{P_f} = \pi - \tan^{-1}\frac{R_f}{h} + \sin^{-1}\left(\frac{R_f + r}{\sqrt{R_f^2 + h^2}}\right)$$

REFERENCES

1. Hanson, D. B.: Near Field Noise of High Tip Speed Propellers in Forward Flight. AIAA Paper 76-565, July 1976.

2. Farassat, F.: Theory of Noise Generation from Moving Bodies with an Application to Helicopter Rotors. NASA TR R-451, 1975.

3. Equations, Tables, and Charts for Compressible Flow. NACA Report 1135, 1953.

4. Energy Consumption Characteristics of Transports Using the Prop-Fan Concept (D6-75780, Boeing Commercial Airplane Co.; NASA Contract NAS2-9104.) NASA CR-137937, 1976.

5. Berenek, Leo L., ed.: Noise and Vibration Control. 1971 McGraw-Hill Book Co., Inc., pp. 174-175.

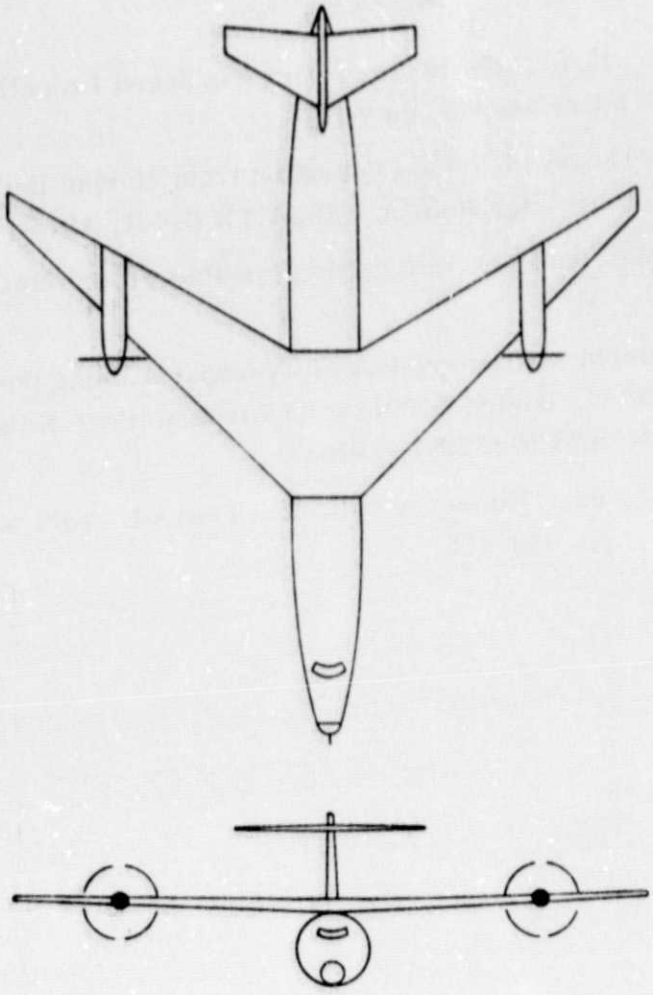

Figure 1. - Turboprop airplane model.

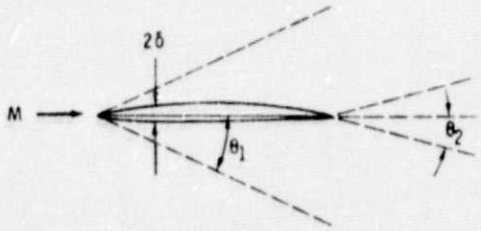

Figure 2. - Blade shock wave angles.

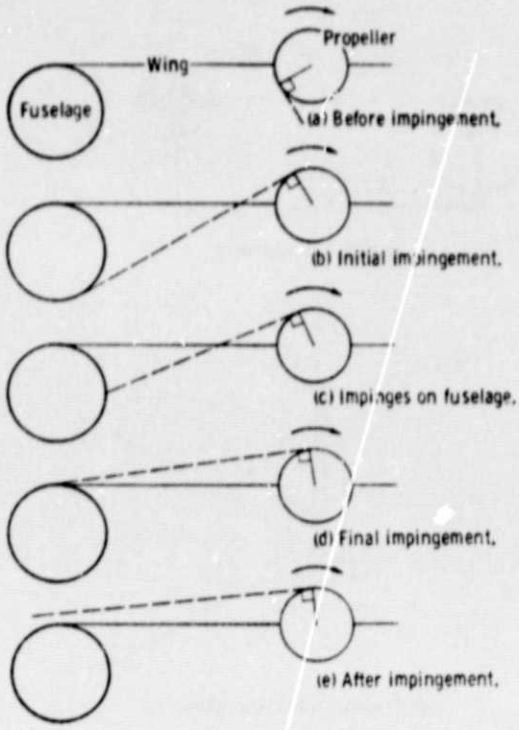

Figure 3. - Suction surface shock wave impingement.

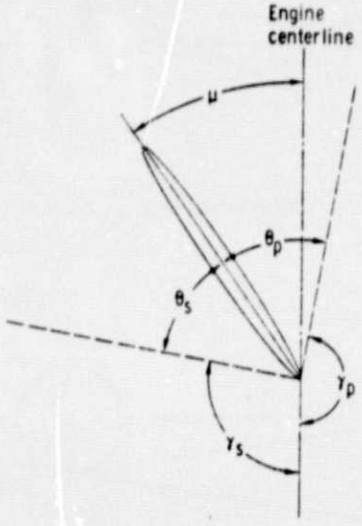

Figure 4. - Relation of shock angles to engine centerline.

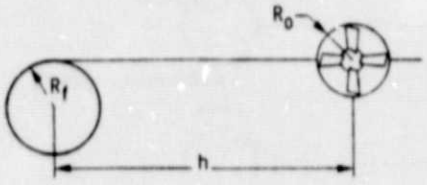

(a) High wing geometry.

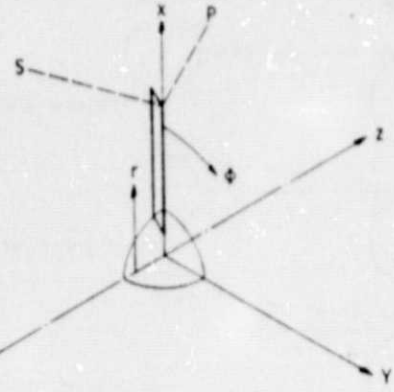

(b) Propeller coordinate system.

Figure 5. - Airplane geometry.

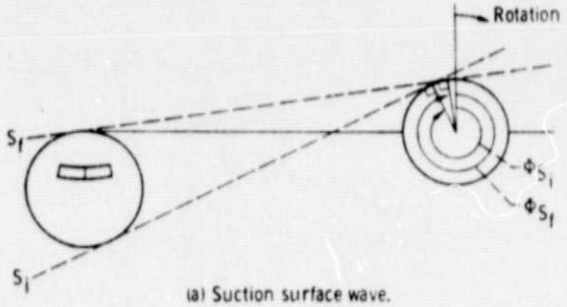

(a) Suction surface wave.

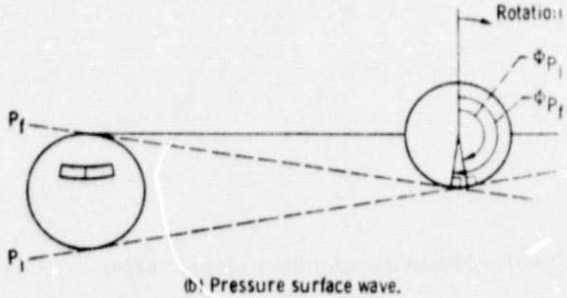

(b) Pressure surface wave.

Figure 6. - Propeller blade positions for initial and final impingement of shock waves.

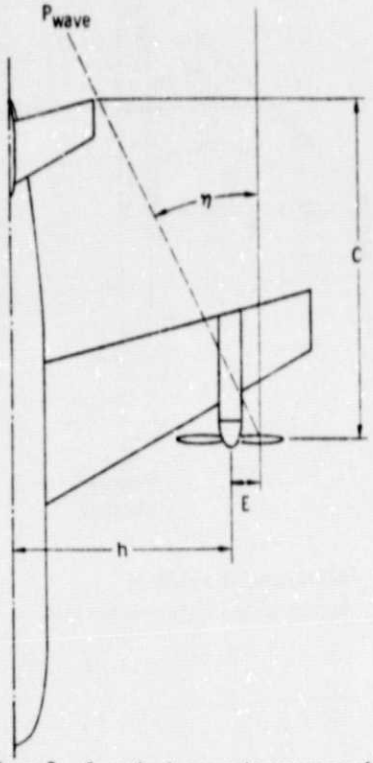

Figure 7. - Geometry to prevent pressure surface shock wave impingement on fuselage.

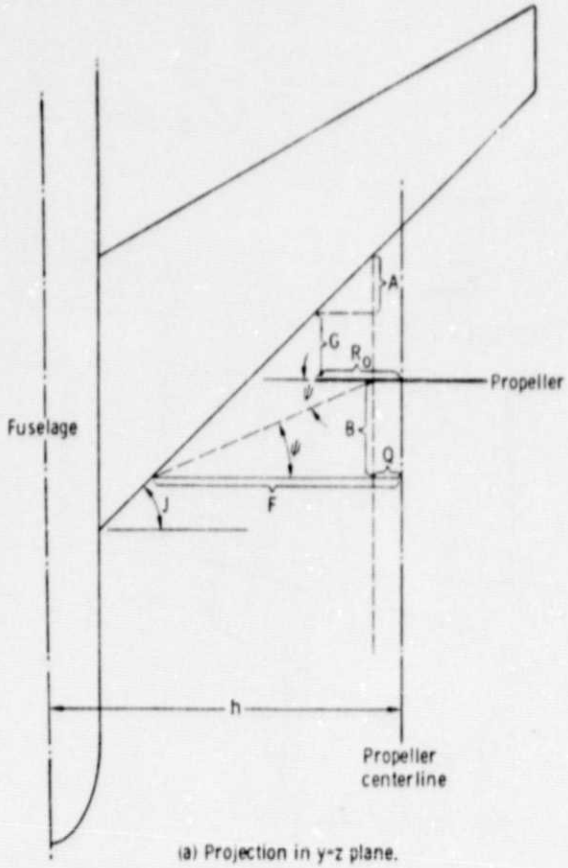

(a) Projection in y-z plane.

Figure 8. - Suction surface shock wave geometry.

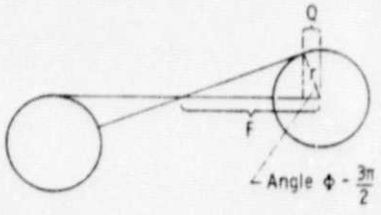

Figure 8b. - Projection in x, y plane.

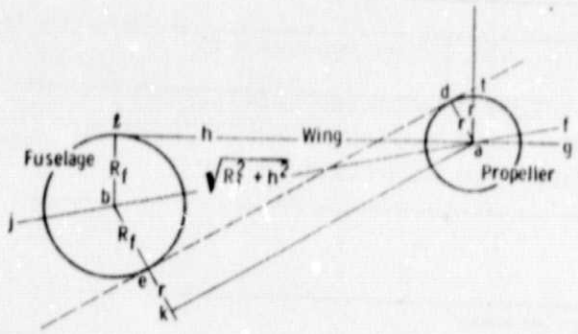

Figure B1. - Solution for Φ_{S_i}

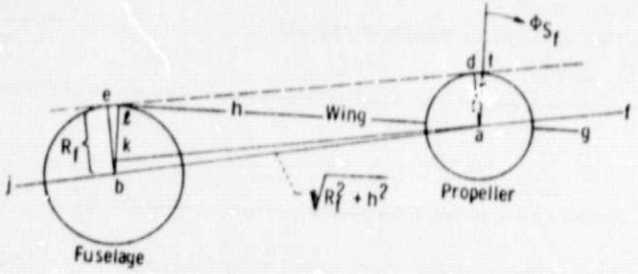

Figure B2. - Solution for Φ_{S_f}

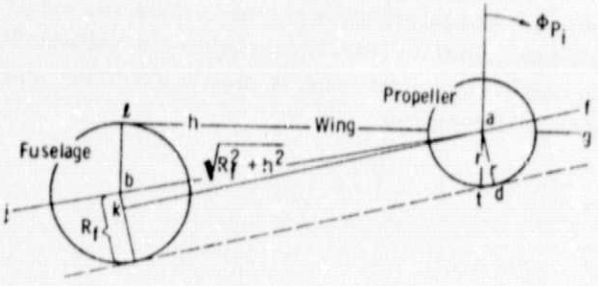

Figure B3. - Solution for Φ_{P_i}

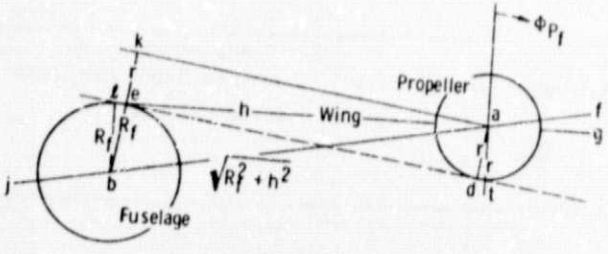

Figure B4. - Solution for Φ_{P_f}